RSC Advances

ROYAL SOCIETY OF CHEMISTRY

www.rsc.org/advances

Facile method to synthesize silver nanoparticles on the surface of hollow glass microspheres and their microwave shielding properties

Zheng Huang[a, b]*, Bo Chi[a], Jianguo Guan[c], Yaqing Liu[b]

[a]*Center for Fuel Cell Innovation, State Key Laboratory of Material Processing and Die & Mould Technology, School of Materials Science and Engineering, Huazhong University of Science & Technology, Wuhan, 430074, China*

[b]*Research Center for Engineering Technology of Polymeric Composites of Shanxi Province, School of Materials Science and Engineering, North University of China, TaiYuan, 030051, China*

[c]*State Key Laboratory of Advanced Technology for Materials Synthesis and Processing, Wuhan University of Technology, Wuhan, 430070, China*

* Corresponding author: Tel /fax: +86 27 87558142

E-mail addresses: hznuc@163.com

Abstract:

In this paper, a facile method for fabrication of hollow glass microspheres/Ag composite particles with core-shell structures is investigated. Ag-coated hollow glass microspheres with raspberry morphology have been prepared by *in-situ* composite technique in the presence of poly -vinylpyrrolidone (PVP). The as-prepared composite particles are characterized by XRD, SEM, EDS, TEM, IR, and XPS. The results show that 3-aminopropyltriethoxysilane (APTS) coupling can remarkably improve the adhesion between the palladium colloid particles and the surface of hollow glass microspheres, increasing the amount of active sites on the surface of hollow glass micropheres. With the increase of pH value, the equilibrium of $[Ag(NH_3)_2]^+$ solution is destroyed and beneficial to the output of Ag nanoparticles. The shell thickness of silver-coated hollow glass microspheres increases from 30 nm to 52 nm with the increase of the concentration of the $[Ag(NH_3)_2]^+$ solution. The shielding property of the composite particles increases gradually and shows an obvious leap in the range of 30% to 35% with increasing the volume fraction of the composite particles. When the volume fraction of the filler reaches 35%, the shielding effectiveness is between 70 dB and 80 dB with the frequency of electromagnetic wave ranging from 2 GHz to 12 GHz. These results indicate that the Ag-coated glass microspheres core-shell particles should have extensive application prospects in the electromagnetic compatibility field.

Keywords: microspheres; nanoparticles; in-situ; chemical deposition; shielding property

1. Introduction

As large use of electronics, communication devices and instruments, interference among devices, such as foldable cellular phones, wearable computers, and radios can degrade their performance [1]. The shielding or block of electromagnetic signals is one effective technique to meet working requirements of such devices, also suggesting the solution for the growing concern from electromagnetic irradiation and interference in the society [2-4]. Many electromagnetic shielding materials such as metals [5], carbon-based materials [6-7], and electrically conducting polymer composites [8-10] have been intensively studied in both fundamental and applied research fields to prevent undersirable effects.

Traditionally, typical metals are considered to be the best material for electromagnetic shielding but they often suffer from the disadvantages of heavy weight and easy corrosion, which restrict wide use of these materials [11]. Carbon-based materials such as carbon nanotubes [12], carbon black [13], and carbon fibers [14] are often used as conducting fillers. Which are incorporated into polymers to make efficient electromagnetic shielding materials that are lightweight, flexible, corrosion resistant, and effective. Nevertheless, the oxidation prone of carbon materials and polymers at low temperature restricts some of their applications when used in oxidizing atmospheres. It is also to be noted that electrically conducting polymers are currently expensive, difficult to process, and need considerable improvements in mechanical properties [15-17]. On the other hand, the use of polymers for housing the electronic device is popular due to it being light weight, flexible and less expensive. But polymers are electrically insulating and transparent to electromagnetic radiation i.e. their inherent electromagnetic shielding effectiveness is practically zero.

Thin sheets or films, two-dimensional (2-D) structures, which hold unique planar properties with remarkable combination advantages in light weight, mechanical flexibility and easy processing, have attacted most attention in electromagnetic shielding coatings on working parts [18]. Park et al. have prepared CNT thin films into polymeric composites by a vacuum bagging process, followed by fabricating into sandwich structures. The as-obtained structures showed increasing electromagnetic shielding by adjusting the layers of the composite films in the range of 2-18 GHz [19]. Wang et al. used screen pringting to fabricate CNT-based films, which exhibited much higher electromagnetic shielding effectiveness than graphite- and carbon black-based films in the megahertz region [20]. In order to shield against electromagnetic interference, various materials are selected for use in different microelectronics devices depending on their shielding effectiveness over different frequency ranges [21-24]. They are also used in microwave applications to avoid interference due to unwanted electromagnetic waves. Thus a number of workers have endeavored to prepare electrically conductive composites as effective electromagnetic shielding materials [25-30].

As the important raw material of electromagnetic shielding materials, Ag powder is widely used in the electron industry and military affairs [31]. However, Ag is noble metal of low abundance. Therefore, the preparation of Ag coated core-shell composite particles is proposed in order to decrease the dosage of Ag and the density of powders [32-35]. The composite particles with hollow structure not only have low density, but also can control the electromagnetic parameters of the electromagnetic materials by adjusting the configuration parameters of the composite particles in a certain range [36-38]. There are many methods of deposition of Ag nanoparticles on the substrates, such as seed-mediated growth technique [39-42], chemical plating

[43], chemical self-assembly monolayer technique [44-49] and so on. However, most of these methods lead to non-autocatalytic metal plating in the bulk solution and result in coarse suspensions that cause major metal precursor consumption and necessity of their regeneration. The uneven distribution or lower metal coverage on the core surface were obtained [50]. What's more, the shell thickness of composite particles can't be controlled easily.

Based on the autocatalytic redox reaction occurring on the interface between solution and hollow glass microspheres, herein, we report a nanostructured composite particle, Ag nanoparticles coated hollow glass microspheres with even and compact shells by in-situ composite technique in the presence of PVP. The core-shell composite particles have good electric properties, shielding effectiveness but without the high cost or weight, which indicates that the Ag-coated hollow glass microspheres should have extensive application prospects in the electromagnetic compatibility field.

2. Experimental results

2.1 Materials

Hollow sodium borosilicate glass spheres with the size range 2.5~100 μm were used as substrates for silver shells deposition, which were purchased from Shanghai Green Sub-Nanoscale Material Co., Ltd. 3-aminopropyltriethoxysilane (APTS) was purchased from Wuhan University Organosilicon New Material Co., Ltd and vacuum distilled before usage. Silver nitrate (Aldrich, 99.9%) and glucose (Aldrich, 99.9%) were used for Ag shells producing via simple chemical reduction. All the other chemicals used in the experiments were obtained from commercial sources as analytical reagents and used without further purification.

2.2 Preparation of Ag-coated hollow glass microspheres

Prior to use, three surface treatment steps were used in order to improve the surface properties of hollow glass microspheres: (1) all the substrates were cleaned by boiling in 10% (wt%) sodium hydroxide solution for 10 min, then filtered and rinsed with deionized water and ethanol, dried at 80 ºC overnight. (2) immersing the as-prepared substrates into APTS coupling agent solution for 2 h and dried at 60 ºC. (3) immersing the as-prepared coupling substrates into colloid palladium activator solution for 4 h and dried at 80 ºC. (according literature [51], in brief, 1.0 g $PdCl_2$ was dissolved in 1000 mL deionized water, then 20 mL HCl (37 wt%) was added under magnetic stirring for 30 min)

For preparation of Ag-coated hollow glass microspheres, Ag nanoparticles were prepared by the reduction of $AgNO_3$ solution in glucose ($C_6H_{12}O_6$) solution in the presence of PVP. 3.5 g $AgNO_3$ was dissolved in 60 mL deionized water, then 0.1 M $NH_3 \cdot H_2O$ (28 wt%) was added until the solution became transparent again to form $[Ag(NH_3)_2]^+$ solution. Reducing solution was prepared by mixing 45 g $C_6H_{12}O_6$, 1.5 g PVP, 100 mL ethanol and 1 L deionized water together. 1.5 g of functionalized hollow glass microspheres was dispersed in 50 mL of 1 wt% sodium dodecyl sulfonate (SDS) of $[Ag(NH_3)_2]^+$ solution for 30 min. Then silver-coated hollow glass microspheres can be obtained by mixing $[Ag(NH_3)_2]^+$ solution and reducing solution with a ratio of 1/1 (v/v) dropwise under magnetic stirring for 6 h. The final products were collected by centrifugation (8000 rpm/10 min), washed with ethanol and deionized water and dried under vacuum at 80 ºC.

2.3 Characterization

To reveal detailed information about the chemical composition and crystallographic structure, powder X-ray diffraction (XRD) was carried out by using an X′ Pert PRO X-ray diffractometer

with CuK_{α} radiation of wavelength 0.154056 nm at a scan speed of $10°min^{-1}$. The surface morphology and structure of composites were examined by transmission electron microscopy (TEM) with a Philips CM12 microscope operated at 80 kV and a field emission scanning electron microscopy (FESEM) with a Zeiss DSM940 instrument operated at an accelerating voltage of 20 kV. The component analysis of the samples was carried out on an Energy Dispersive Spectroscopy (EDS). The function group of composite particles were examined by infrared (IR) with scanning in the range of 4000 cm^{-1} to 400 cm^{-1}. The compositions of composite particles were examined by X-ray photoelectron spectroscopy (XPS) (Perkin-Elmer, PHI-5300) using MgKα source at 1253.6 eV. The X-ray powder supply was operated at 250 W (12.5 kV 20 mA). The pressure in the analysis chamber during scans was kept below 2×10^{-7} Pa.

2.4 Electrical conductivity and EMI shielding measurement

The volume resistivity (ohmcm) of composites with a high resistivity $\geq10^{8}$ ohmcm was measured using Hewlett-Packard high resistance meter (model 4329A) coupled with a Hewlett-Packard (model 160084) resistivity cell. For composites having low resistivity, the volume resistivity was measured by a four-probe technique using the Vander Pauw method as described in the literature [52]. To measure the volume resistivity at a constant temperature, the entire electrode system was placed in an oven where the temperature could be monitored and controlled. The resistivity data used were the average of results of three samples (samples were produced as well-dispersed mixtures at the same volume percent using solid paraffin).

The complex permittivity of 2~12 GHz was determined with a coaxial cell on a Hewlett-Packard 8510C Vector Network Analyzer. The core-shell particles were processed as well-dispersed mixtures, respectively. For example, the mixtures containing 30% (in volume, the

same below) core-shell microspheres sample and 70% solid paraffin as an adhesive resulted in the coaxial cylindrical samples with the following characteristics: outer diameter of 7.00 mm, inner diameter of 3.02 mm and thickness of about 3.5 mm. The shielding effectiveness of the coating was measured according to ASTM-ES-7. A network analyser (4396B; Agilent Technologies, Inc., Santa Clara, CA, USA) and an S-Parameter test set (Agilent; 85046A) were employed. A coaxial sample holder was designed according to ASTM D4935-10. The electromagnetic shielding coating were processed by mixing various quantities of shielding filler (Ag coated hollow glass microspheres) into epoxy resin adhesive. Then the coating samples were processed at 100 ºC for 10 h. The diameter of the load specimen was 13.5 cm.

3. Results and discussion

Fig.1 shows the schematic illustration of the formation process of Ag nanoparticles decorating hollow glass microspheres. It has been demonstrated that glass microspheres tends to carry negative charges in a basic solution due to its isoelectric point (IEP) at ~2 and its zeta potential profile [16]. APTS silane coupling has two functional groups, ethoxy group and amino group. Generally, the chemical deposition reaction of Ag occurs at the adsorbed palladium catalytic active centers on the nonmetallic substrates [53]. The surface of hollow glass microspheres with large amount of hydroxyl groups can interact with ethoxy groups of silane couping via hydrogen bonds. Meanwhile, another amino groups, which have a pair of unbonded electrons could complex with Pd^{2+} whose outside electron figuration is $4d^{8}5s^{0}5p^{0}$. Such bridging function of APTS silane coupling can remarkably improve the adhesion between the palladium colloid particles and the surface of hollow glass microspheres, increasing the amount of active sites on the surface of hollow glass micropheres.

Fig.2 displays the EDS spectrum of the hollow glass microspheres after colloid palladium activator with and without APTS silane coupling. It can be found that the palladium surface content of hollow glass microspheres pretreated with APTS silane coupling exceeds that without pretreament. The surface property of hollow glass microspheres pretreated by APTS silane coupling agent is beneficial for the adsorption of palladium. Therefore, it leads to an increase of the active sites on the surface of hollow glass microspheres and forms an ideal deposition on the hollow glass microspheres.

Fig.3 shows IR spectra of hollow glass microspheres coupled by different concentrations of APTS (0, 0.001, 0.002, 0.003 $mol \cdot L^{-1}$). The intensity of absorbing apex weakened at 3400 cm^{-1} and 1600 cm^{-1} with the increase of the concentrations of APTS, in another word, the quantity of physical absorbing water and Si-OH group decreased. The absorbing apex of CH_2 is observed clearly at 1630 cm^{-1} and the absorbing apex of C=N appears at 1550 cm^{-1} after hollow glass microspheres are coupled by APTS silane coupling agent. It indicates that the surface of hollow glass microspheres really were coupled. The characteristic absorbing apex of SiO_2 (1100 cm^{-1}, 797 cm^{-1} and 471 cm^{-1}) don't have distinct changes. The flex vibration absorbing apex of Si-O strengthened. The physical form and crystal configuration of hollow glass microspheres can't be changed by adding APTS silane coupling agent. It's only that the partial hydroxide group has function with silane coupling to create Si-O bond.

XRD patterns of Ag decorated hollow glass microspheres with APTS silane coupling agent under different pH value (12, 12.5, 13, 13.5, 14) are shown in Fig.4. The pH value of the solution is adjusted by NaOH solution. It can be seen that Ag decorated hollow glass microspheres diffraction peaks around 38.10°, 44.26°, 64.44°, 77.42° are also found for Ag(111), Ag(200),

Ag(220), Ag(311), respectively, which indicates that the metal Ag has been decorated on hollow glass microspheres. The 2θ angle accords with the normal 2θ angle of Ag by contrasting normal card. It indicates that Ag nanoparticles decorating on the surface of hollow glass microspheres have intact face-centred cubic structure. Because there exists an equilibrium in $[Ag(NH_3)_2]^+$ solution with instability coefficient K_β=107.05, so the concentration of Ag^+ in $[Ag(NH_3)_2]^+$ solution is very low during the coating process. When the reducing solution is added to the $[Ag(NH_3)_2]^+$ solution, a small portion of Ag^+ in the solution can be reduced. Ag seed nanoparticles can be formed localized nucleation sites of the surface of hollow glass microspheres. With increase of pH value, the equilibrium is destroyed. The output of Ag becomes more, and the diffracted intensity of Ag becomes stronger.

The samples purity and elemental composition are determined by XPS [35]. Fig.5 shows the XPS spectra for Ag/hollow glass microspheres composite. The binding energies obtained in the XPS analysis are standardized for specimen charging using C1s as the reference at 284.6 eV. No peaks of other elements except C, O, Si and Ag are observed on the survey spectrum. The binding energies are 368.26 eV for $Ag3d_{5/2}$, 103.36 eV for Si2p and 532.56 eV for O1s, respectively. These are assigned to the elements in silica and Ag metal.

Pretreatment method is used in order to obtain ideal chemical deposition of Ag nanoparticles on hollow glass microspheres. The main pretreatment includes surface treatment, APTS silane coupling, colloid palladium activating. Fig.6 shows the typical SEM photographs of with and without Ag nanoparticles decorating the hollow glass microspheres prepared via pretreatment. It is found from Fig.6a that some rough holes appear on the shell of hollow glass microspheres and some broken glass microspheres can be observed. Fig.6b shows that a few Ag nanoparticles

decorate hollow glass microspheres, which are pretreated by colloid palladium activating without APTS silane coupling. Fig.6c show that lots of Ag nanoparticles decorate on the hollow glass microspheres, which are pretreated by colloid palladium activating with APTS silane coupling (the same as above pretreatment). The amounts of palladium increase with APTS silane coupling. In order to investigate the element composition, Ag nanoparticles decorating hollow glass microspheres are analyzed by EDS, as shown Fig.6d. It can be found that the composition of Ag, Si, O, Mg, Al can be observed in the sample and the elements of Si, O, Mg, Al are assigned to hollow glass microspheres. No other impure element is detected,which is almost consistent with the XRD results.

Fig.7 shows the effect of the concentration of $[Ag(NH_3)_2]^+$ solution on the shell thickness of Ag-coated hollow glass microspheres in the presence of PVP. The pristine hollow glass microspheres appear slick sphericity while the composite particles appear raspberry morphology. The shell thickness is about 30 nm when the concentration of $[Ag(NH_3)_2]^+$ solution is 0.2 M. Ag nanoparticles are produced more and more with the increase of the concentration of $[Ag(NH_3)_2]^+$ solution. The renascent Ag nanoparticles have very high activity and the subsequent Ag nanoparticles are formed on the interfaces which have high active potential location. So the size of Ag-coated hollow glass microspheres become larger and larger. The shell thickness of silver-coated hollow glass microspheres increases from 30 nm to 52 nm with the increase of the concentration of $[Ag(NH_3)_2]^+$ solution.

Fig.8 shows the electromagnetic shielding effectiveness curve of mixture with different volume fraction of particles in the range of 2.0 GHz to 12.0 GHz. Compared to coating material with excessive volume fraction for fillers, inadequate fillers will lead to inferior electric properties

of the coating. According to Schelkunoff theory, shielding material with perfect electric properties will have perfect electromagnetic shielding properties. The perfect electric properties contribute to strong reflection and absorbance losses in the shielding effectivess of electromagnetic shielding material. With increasing volume fraction of composite particles, the shielding effectiveness of composites increases gradually and shows an obvious leap in the range of 30% to 35%. The conductive particles can't form catenarian morphology in the mixture with decreasing the volume fraction of particles. When volume fraction of particles increase, the particles can't form effective conductive net due to loose structure of the mixture.

4. Conclusions

In summary, a facile method for fabrication of hollow glass microspheres/Ag composite particles with core-shell structures is investigated. Ag-coated hollow glass microspheres with raspberry morphology have been prepared by *in-situ* composite technique in the presence of PVP. The as-prepared composite particles are characterized by XRD, SEM, EDS, TEM, IR, and XPS. The results show that 3-aminopropyltrimethoxysilane (APTS) coupling can remarkably improve the adhesion between the palladium colloid particles and the surface of hollow glass microspheres, increasing the amount of active sites on the surface of hollow glass micropheres. With the increase of pH value, the equilibrium of $[Ag(NH_3)_2]^+$ solution is destroyed and it is beneficial to the output of Ag nanoparticles. The shell thickness of silver-coated hollow glass microspheres increases from 30 nm to 52 nm with the increase of the concentration of the $[Ag(NH_3)_2]^+$ solution. The shielding property of the composite particles increases gradually and shows an obvious leap in the range of 30% to 35% with increasing the volume fraction of the composite particles. When the volume fraction of the filler reaches 35%, the shielding effectiveness is between 70 dB and 80 dB with the

frequency of electromagnetic wave ranging from 2 GHz to 12 GHz. These results indicate that the Ag-coated glass microspheres core-shell particles should have extensive application prospects in the electromagnetic compatibility field.

Acknowledgments

The authors would like to thank Program for National Ministry of Education "New Century Excellent Person with Ability Auspice Program" (No.WCET-05-0660) for financial support and Materials Characterization Center of Wuhan University of Technology and North University of China for samples characterization assistance.

Reference

[1] N. C. Das, D. Khastgir, T. K. Chaki, A. Chakraborty, *Composites: Part A*., 2000, 31, 1069−1081.

[2] T. K. Gupta, B. P. Singh, R. B. Mathur, S. R. Dhakate, *Nanoscale.,* 2014, 6, 842−851.

[3] F. Ye, L.-T. Zhang, X.-W. Yin, X.-F. Liu, Y.-S. Liu, J.-M. Xue, L.-F. Cheng, *J. Alloy. Compd*., 2014, 589, 579−589.

[4] H. Azizi, F. T. Belkacern, D. Moussaoui, H. Moulai, A. bendaoud, M. Bensetti, *J. Electromagn. waves Appl*., 2014, 28, 494−514.

[5] M. Yang, W.-C. Zhou, F. Luo, D.-M. Zhu, Y.-C. Qing, Z.-B. Huang, *J. Mater Sci*., 2014, 49, 1527−1536.

[6] T. W. Yoo, Y. K. Lee, S. J. Lim, H. G. Yoon, W. N. Kim, *J. Mater Sci*., 2014, 49, 1701−1708.

[7] S. Varshney, A. Ohlan, V. K. Jain, V. P. Dutta, S. K. Dhawan, *Mater. Chem. Phys*., 2014, 143, 806−813.

[8] A. Das, J. Krishnasamy, R. Alagirusamy, A. Basu, *Fiber. Polym*., 2014, 15, 169−174.

[9] X.-C. Wang, Z. Liu, Z. Zhou, *Int. J. Appl. Electromagn. Mech*., 2014, 44, 87−97.

[10] D. Soyaslan, O. Goktepe, S. Comlekci, *Sci. Eng. Compos. Mater*., 2014, 21, 129−135.

[11] Y.-M. Wang, *Int. J. Mater. Res*., 2014, 105, 3−12.

[12] M. S. Kim, J. Yan, K. H. Joo, J. K. Pandey, Y. J. Kang, S. H. Ahn, *J. Appl. Polym. Sci*., 2013, 130, 3947−3951.

[13] T. Zhai, L.-Z. Di, D.-A. Yang, *ACS Appl. Mater. Interfaces*., 2013, 5, 12499−12509.

[14] W.-L. Song, M.-S. Cao, M.-M. Liu, B. Song, C.-Y. Wang, J. Liu, J. Yuan, L.-Z. Fan, *Carbon*., 2014, 66, 67−76.

[15] W.B. Ko, Y. J. Oh, B. H. Cho, *Asian J Chemistry*., 2013, 25, 4657−4660.

[16] W. Wang, Z.-P. Li, B.-H. Gu, Z.-Y. Zhang, H.-X. Xu, *ACS NANO*., 2009, 3, 3493−3496

[17] B. Zhang, L.-P. Zheng, W.-Y. Li, J.-W. Wang, *Curr. Nanosci*., 2013, 9, 363−370.

[18] X.-S. Zhang, J.-X. Wang, K. Xu, Y.-A. Le, J.-F. Chen, *J. Nanosci. Nanotechnol*., 2011, 11, 3481−3487.

[19] J. G. Park, J. Louis, Q. Cheng, J.-W. Bao, J. Smithyman, R. Liang, *Nanotechnol*., 2009, 20, 1−7.

[20] L.-L. Wang, B. K. Tay, K. Y. See, Z. Sun, L. K. Tan, D. Lua, *Carbon*, 2009, 47, 1905−1910.

[21] A. Kudelski, S. wojtysiak, *J. Phys. Chem. C*., 2012, 116, 16167−16174.

[22] L. V. Mathieu, D. Brouard, *J. Phys. Chem. C*., 2011, 115, 2974−2981.

[23] S. Okada, S. Ikurumi, T. kamegawa, K. Mori, H. Yamashita, *J. Phys. Chem. C*., 2012, 116, 14360−14367.

[24] C.-Y. Li, Y.-H. Zhu, X.-Q. Zhang, X.-L.Yang, C.-Z. Li, *RSC Adv*., 2012, 2, 1765−1768.

[25] J. C. Flores, V. Torres, M. Popa, D. Crespo, J. M. Calderon, *J Non-Cryst. Solids*., 2008, 354,

52−54.

[26] M. L. Viger, L. S. Live, O. D. Therrien, D. Boudreau, *Plasmonics*., 2008, 3, 33−40.

[27] B. P. bastakoti, S. Guragain, S. Yusa, K. nakashima, *RSC Adv.*, 2012, 2, 5938−5940.

[28] B.-L. Lv, Y. Xu, H. Tian, D. Wu, Y.-H. Sun, *J. Solid State Chem*., 2010, 183, 2968−2973.

[29] F. Tang, F. He, H.-C. Cheng, L.-D. Li, *Langmuir*, 2010, 26, 11774−11778.

[30] P.-Y. Yuan, Y.-H. Lee, Z.-P. Guan, Q.-H. Xu, *Nanoscale*., 2012, 4, 5132−5137.

[31] D. Mongin, V. Juve, P. Maioli, A. Curt, F. Vallee, *Nano Lett*., 2011, 11, 3016−3021.

[32] G.-X. Gu, J.-X. Xu, Y.-F. Wu, M. Chen, L.-M, Wu, *J. Colloid Interface Sci*., 2011, 359, 327−333.

[33] J. P. Yang, F. Zhang, Y.-R. Chen, S. Qian, P. Hu, W. Li, Y.-H. Deng, *Chem. Commun*., 2011, 47, 11618−11620.

[34] T. Liu, D.-S. Li, D.-R.Yang, M.-H. Jiang, *Chem. Commun*. 2011, 47, 5169−5171.

[35] T.-Y. Zhang, X.-Q. Li, S.-Z. Kang, L.-X. Qin, G.-D. Li, J. Mu, *J. Mater. Chem. A*, 2014, 2, 2952-2959.

[36] J.-J. Liang, Y. Wang, Y. Huang, Y.-F. Ma, Z.-F. Liu, J.-M. Cai, C.-D. Zhang, H.-J. Gao, Y.-S. Chen, *Carbon*, 2009, 47, 922−925.

[37] S. Kwon, R.-J. Ma, U. Kim, H. R. Choi, S. Baik, *Carbon*. 2014, 68, 118−124.

[38] W.-L. Song, P. Wang, L. Cao, A. Anderson, M. J. Meziani, A. J. Farr, *Angew Chem Int Ed*. 2012, 51, 6498−6501.

[39] M.-J. Hu, J.-F. Gao, Y.-C. Dong, K. Li, G.-C. Shan, S.-L. Yang, *Langmuir*. 2012, 28, 7101−7106.

[40] D.-X. Yan, P.-G. Ren, H. Pang, Q. Hu, M.-B. Yang, Z.-M. Li, *J Mater Chem*, 2012, 22,

18772−18774.

[41] W.-L. Song, M.-S. Cao, M,-M. Lu, J. Yang, H.-F. Ju, Z.-L. Hou, *Nanotechnol.*, 2013, 24, 115708(1-10).

[42] P. Saini, V. Choudhary, N. Vijayan, R. K. Kotnala, *J Phys Chem C*, 2012, 116, 13403−13412.

[43] X.-M. Kong, Q. Yu, X.-F. Zhang, X.-Z. Du, H. Gong, *J. Mater. Chem*., 2012, 22, 7767−7774

[44] B. S. Villacorta, T. H. Hubing, A. A. Ogale, *Compos. Sci. Technol*, 2013, 89, 158−166.

[45] G. Mondin, F. M. Wisser, A. Leifert, N. N. Mohamed, J. Grothe, S. Dorfler, S. Kaskel, *J. Colloid Interface Sci.*, 2013, 411, 187−193.

[46] J. A. Andres, N. P. Gonzalez, C. Fonseca, E. Perez, M. L. Cerrada, *Mater. Chem. Phys*, 2013, 142, 2−3.

[47] B. Shen, W.-T. Zhai, M.-M. Tao, J.-Q. Ling, W.-G. Zheng, *ACS Appl. Mater. Interfaces*, 2013, 5, 11383−11391.

[48] S. Ryu, C. B. Mo, H. Lee, S.-H. Hong, *J. Nanosci. Nanotechnol*, 2013, 13, 7669−7674.

[49] S. G. Pardo, L. Arboleda, A. Ares, X. Garcia, S. Dopico, M.-J. Abad, *Polym. Compos*, 2013, 34. 1938−1949.

[50] L.-Y. Zhang, L.-B. Wang, K. Y. See, J. Ma, *J. Mater. Sci*, 2013, 48, 7757−7763.

[51] R. K. Goyal, *Mater. Chem. Phys*, 2013, 142, 195−198.

[52] Arranz-Andres. J, E. Perez, M. L. Cerrada, *Sci. Adv. Mater*, 2013, 5, 1524−1532.

[53] J. Huang, Q. Li, Denian. Li, Y. wang, L.-J. Dong, H. –A. Xie, J. Wang, C.-X. Xiong, *Langmuir*, 2013, 29, 10223−10228.

Figure captions

Fig.1. A schematic illustration of the procedure for generating silver decorated hollow glass microspheres

Fig.2. EDS spectrum of pretreated hollow glass microspheres with and without coupling

Fig.3. IR spectra of hollow glass microspheres coupled by different concentrations of APTS. (a) 0, (b) 0.001mol·L^{-1}, (c) 0.002 mol·L^{-1}, (d) 0.003 mol·L^{-1}.

Fig.4. XRD patterns of silver-coated hollow glass microspheres obtained under different pH

Fig.5. XPS analysis of silver coated hollow glass microspheres

Fig.6. Morphology of hollow glass microspheres with and without silver nanoparticles decorating. (a) etched by sodium hydroxide; (b) reaction for 4 h without coupling; (c) reaction for 8h with coupling and EDS spectrum of composite particles

Fig.7. TEM photographs of silver coated hollow glass microspheres obtained under different concentrations of $[Ag(NH_3)_2]^+$ in the presence of PVP. (a) 0, (b) 0.2 mol·L^{-1} (c) 0.4 mol·L^{-1} (d) 0.6 mol·L^{-1}

Fig.8. The shielding effectiveness curve of mixtures with different volume fraction under the frequency of microwave ranging from 2.0 GHz to 12.0 GHz.

Fig.1

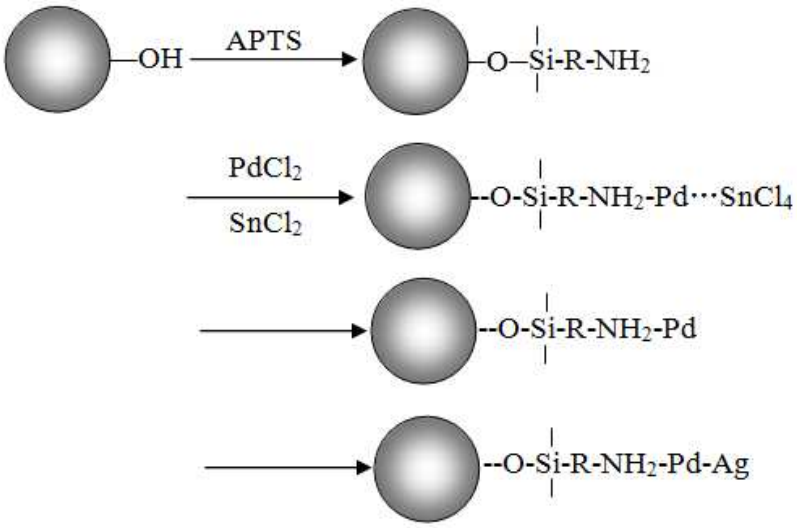

Fig.2

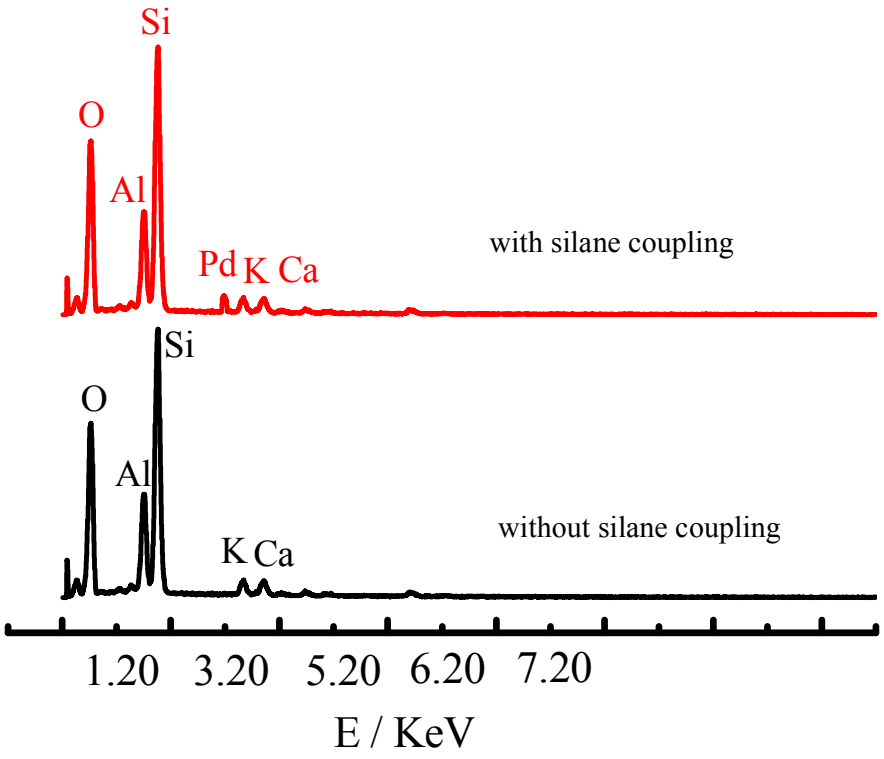

Fig.3

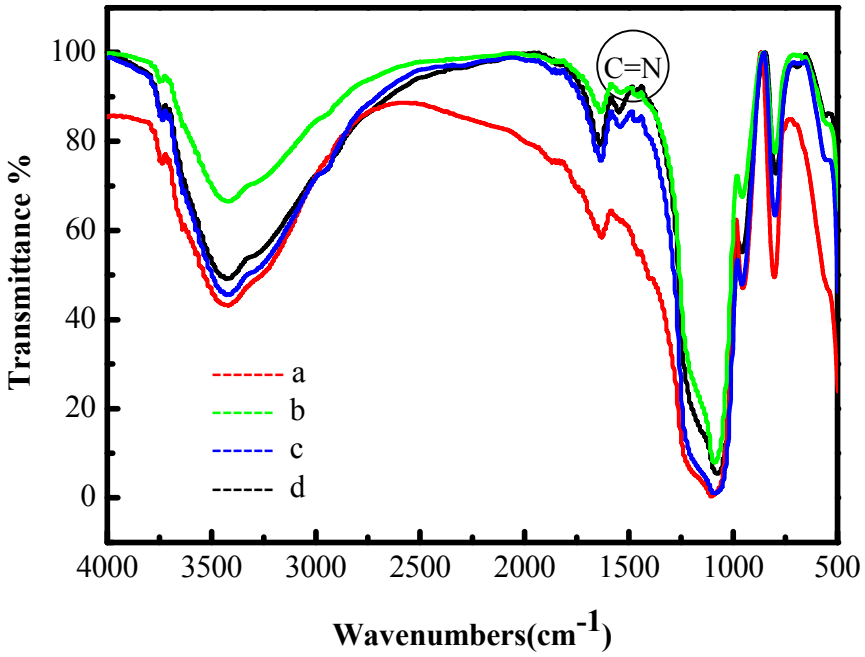

Fig.4

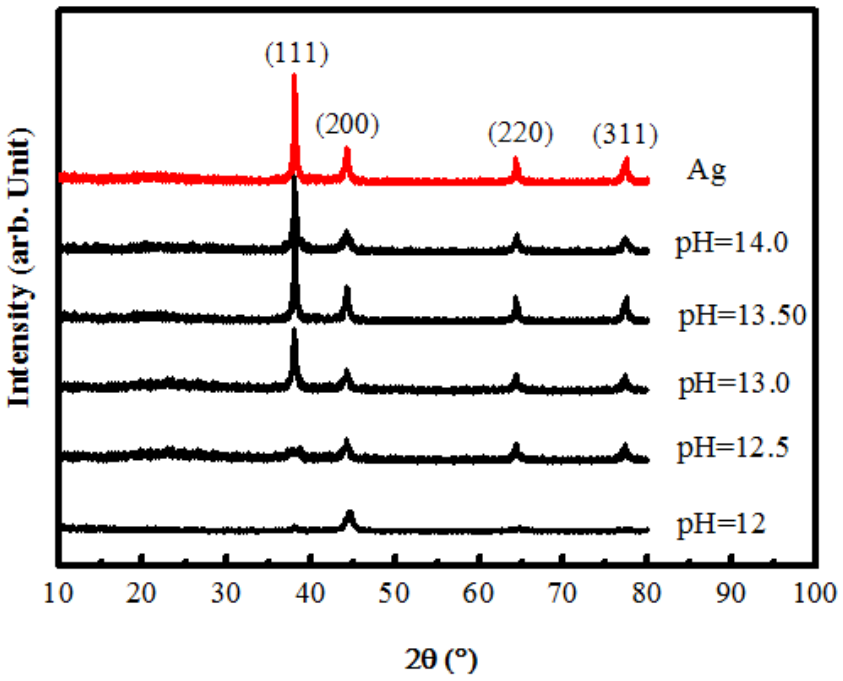

Fig.5

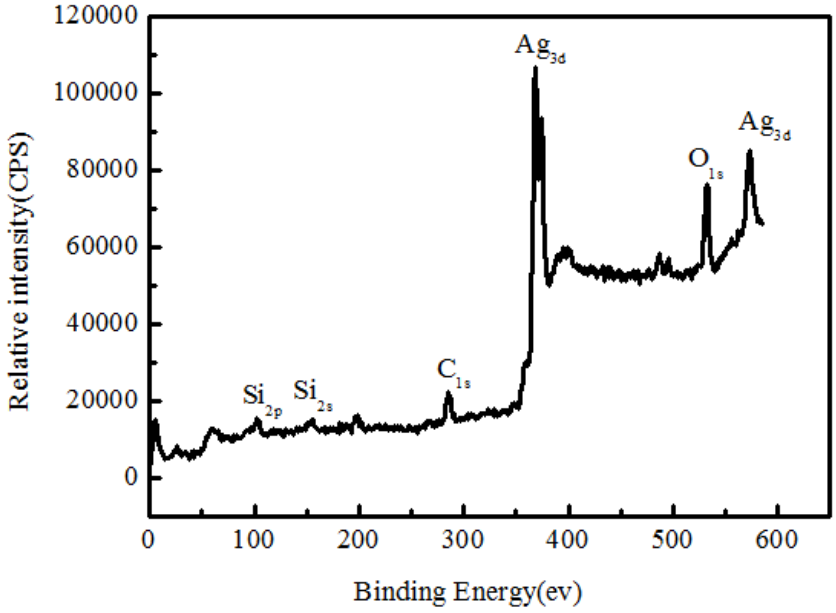

Fig.6

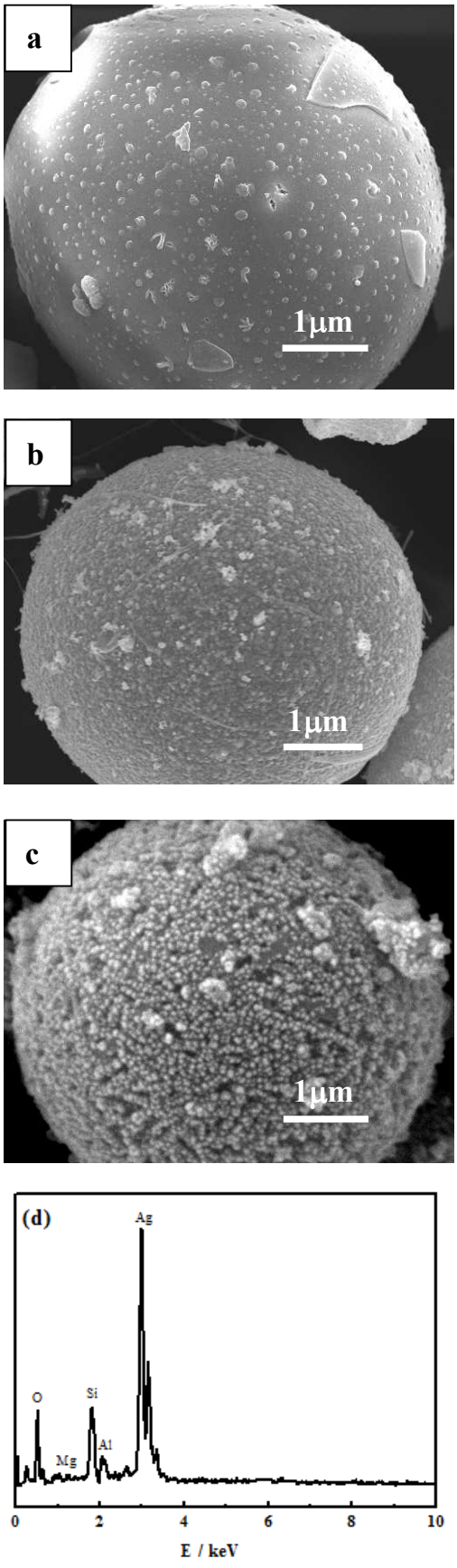

Fig.7

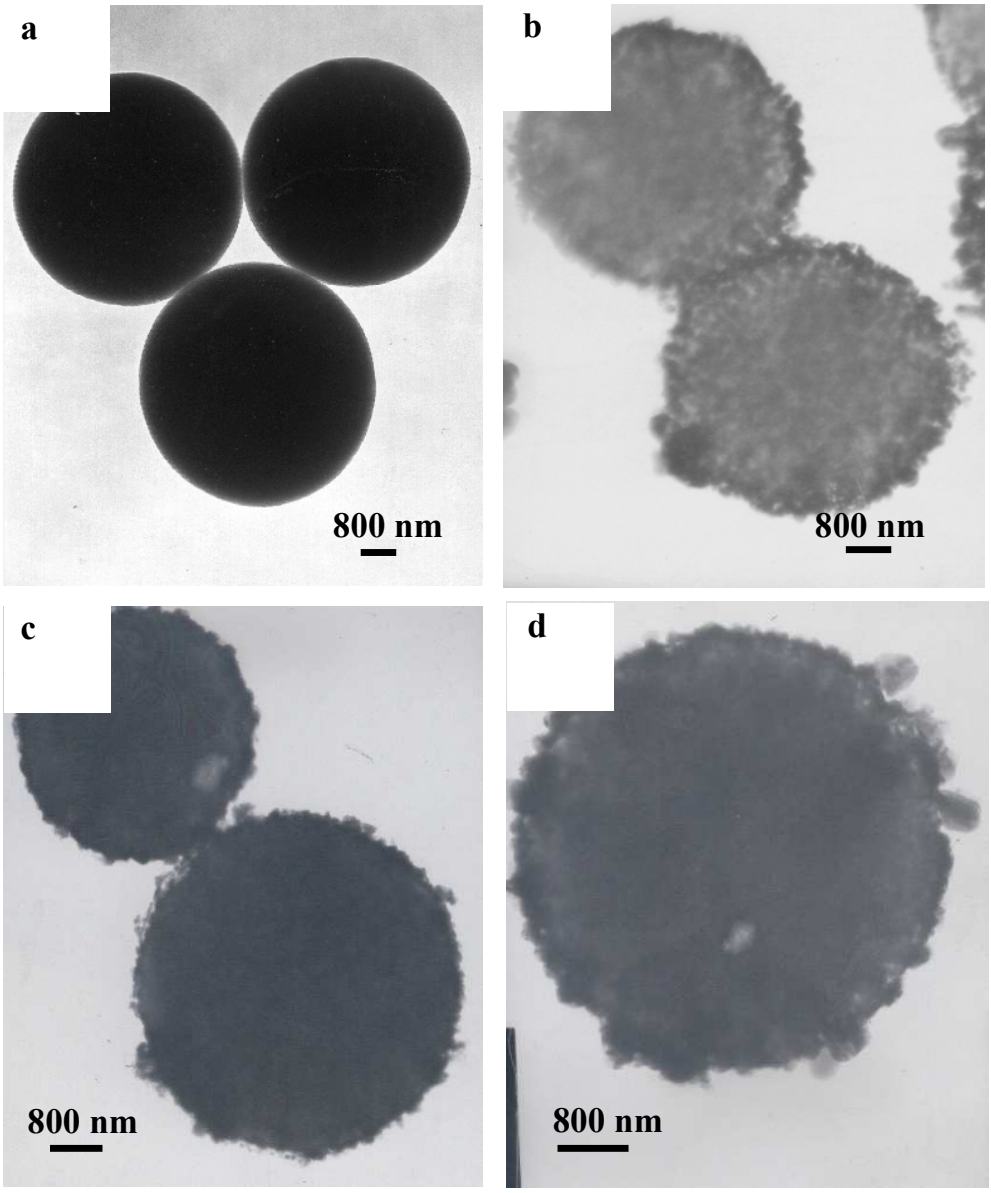

Fig.8